Functional Materials 20, No.1 (2013)

Phase transitions in the nanopowders $KTa_{0.5}Nb_{0.5}O_3$ studied by Raman spectroscopy

I.S.Golovina, V.P.Bryksa, V.V.Strelchuk, I.N.Geifman[*]

Institute of Semiconductor Physics, National Academy of Sciences of Ukraine, 41 Nauki Ave., 03028 Kyiv, Ukraine
[*]Quality Engineering Education, Inc., Buffalo Grove, IL 60089, USA

Received October 10, 2012

Raman spectra of $KTa_{0.5}Nb_{0.5}O_3$ nanopowder solid solution were obtained at the temperatures from −190°C to 600°C and investigated for the first time. The compound was synthesized by a new technology. Temperature dependences of the intensity, width and frequency of the $B_1(TO_2)$, $A_1(TO_1)$, $B_1(TO_3)$, $A_1(TO_3)$ and $B_2(TO_3)$ modes are thoroughly analyzed. A significant expanding of the temperature ranges of all phase transitions, correlated with a spread of particle sizes is registered. It was found that an average temperature of each of the phase transitions is shifted in different way, in particular: a low-temperature transition at 30 degrees higher, the middle transition at 10 degrees higher, and the ferroelectric phase transition occurs at 20 degrees lower than the temperature of the corresponding transitions in single-crystal $KTa_{0.5}Nb_{0.5}O_3$.

Впервые получены и исследованы Рамановские спектры нанопорошков твердого раствора $KTa_{0.5}Nb_{0.5}O_3$ в диапазоне температур $-190°C<T<600°C$. Материал синтезирован по новой технологии. Температурные зависимости интенсивности, ширины и частоты мод $B_1(TO_2)$, $A_1(TO_1)$, $B_1(TO_3)$, $A_1(TO_3)$ и $B_2(TO_3)$ тщательно проанализированы. Зарегистрировано существенное размытие областей всех фазовых переходов, связанное с разбросом частиц по размерам. Установлено, что средние температуры областей каждого из фазовых переходов сдвигаются различным образом, а именно: низкотемпературный переход осуществляется на 30 градусов выше, средний — на 10 градусов выше, а сегнетоэлектрический переход происходит на 20 градусов ниже температур соответствующих переходов в монокристаллах $KTa_{0.5}Nb_{0.5}O_3$.

1. Introduction

Due to the high electro-optical and nonlinear optical coefficients, solid solutions $KTa_{1-x}Nb_xO_3$ (KTN) are attractive optical materials, in particular for light modulators, optical deflectors and waveguides, frequency multipliers, holographic memory systems, etc. [1–5]. Because these materials are lead-free, they are also alternatives to lead-containing materials that are currently used in most ultrasonic applications. Recently, special attention has been paid to the research of size effects observed in film samples of solid solutions $KTa_{1-x}Nb_xO_3$ [6–9]. These effects are manifested primarily in the shift of phase transition temperatures. Particularly important is the knowledge of the ferroelectric phase transition temperature (i.e., the Curie temperature), because exactly in this transition region that materials are effective for practical applications. It is known that in large single crystals $KTa_{1-x}Nb_xO_3$ (with niobium concentration of more than 20 mol.%) we observe the following sequence of phase transitions with increasing temperature: Rhombohedral (R) → Orthorhombic (O) → Tetragonal (T) → Cubic (C), where P-, O- and T-phases are ferroelectric, and C is the paraelectric phase. And, as it has been established by S.Triebwasser [10], there is almost linear increase of temperatures of all three transitions, and also

increase of the intervals between them with increasing content of niobium in the solid solution. To date, the results on the effect of crystal size on these temperatures are ambiguous and therefore have not been systematized yet. A.Bartasyte et al. [6] in the study of thin films of mixed compositions $KTa_{1-x}Nb_xO_3$ with $x = 0.35$ and 0.5 found the same sequence of phase transitions like it was observed in the single crystals, but the Curie temperature (T_c) was 50 degrees higher than in the single crystals. The authors attribute the T_c increase to the existence of biaxial stress, which is created during the growth of the films. The film thickness was 300 nm. In [7], in the study of heterostructures $KTaO_3/KNbO_3$ it is found that by decreasing the thickness of the layer of $KNbO_3$ to 17 nm the Curie temperature becomes 535°C, i.e. 100 degrees higher than in single-crystal $KNbO_3$. Further reduction in the thickness of $KNbO_3$ to 5 nm or less leads to such a change in the properties of the heterostructure $KTaO_3/KNbO_3$, that it behaves like a thin film solid solution $K(Ta_{0.5}Nb_{0.5})O_3$. The Curie temperature of such a heterostructure, T_c=202°C [8], is also almost 100 degrees higher that in single-crystal $KTa_{0.5}Nb_{0.5}O_3$ (T_c = 105°C). These data refer only to studies of the single-crystal films. However, in [11], in the study of polycrystalline thin films of $Ba_{0.5}Sr_{0.5}TiO_3$ a decrease of T_c is observed. The authors suggest that this is due to the influence of the microcrystals sizes. It should be noted that only the group of Chinese researchers has obtained nano-sized KTN powders very recently. Description of the synthesis and structure of these samples are presented in [12–14]. The properties of these materials have not been studied yet. Thus, to date there are no data on the size effect (at the nano-scale level) in powder samples $KTa_{0.5}Nb_{0.5}O_3$. In addition, as can been seen from the above works, there is a few data on the effect of particle size on the phase transition temperature in the film samples of $KTa_{0.5}Nb_{0.5}O_3$ solid solutions. Therefore, the development of a new synthesis technology and the investigation of size effects on these objects are topical. In our previous work we studied the nanopowders of pure $KNbO_3$, synthesized by the technology developed by A.A.Andriiko's group [15].

In this paper, a similar technology was used to synthesize a mixed compound $KTa_{0.5}Nb_{0.5}O_3$ for the first time. It was established that the obtained powders have dimensions less than 100 nm, and therefore belong to nanocrystalline objects. First of all, we set a goal of establishing the phase transition temperatures of the synthesized powders. To solve this problem we selected Raman scattering method. This technique is the most suitable for such objects, because, on the one hand, it does not require the high-density ceramic, in contrast to the dielectric spectroscopy, and on the other hand, it is quite informative. We carried out a detailed study of the temperature dependence of Raman scattering spectra for synthesized powders $KTa_{0.5}Nb_{0.5}O_3$. We analyzed data and determined the phase transition temperatures.

2. Experimental

There was recently developed a method of synthesis of $KTaO_3$ by oxidation of metal tantalum in molten potassium nitrate with the addition of potassium hydroxide. It was shown that this method can be used to obtain nano-sized powders [15–17]. In this paper, the same method has been used to synthesize powders of solid solutions $KTa_{1-x}Nb_xO_3$ with niobium concentration $x = 0.5$. The masses of the initial components used were follows: Ta = 0.66 g, Nb = 0.34 g, KOH = 0.49 g, KNO_3 = 7.37 g. Weighed portions of the initial components were mixed and grinded. The mixture was then placed in a furnace and melted at 600°C for 1.5 h. The resulting melt was cooled in air and decanted in water. The precipitate was dried at a temperature of 100°C in open air.

The product was investigated by X-ray diffraction (XRD) method on a diffractometer DRON-3M with $Cu_{K\alpha}$ radiation. The results confirmed the formation of compound $KTa_{0.5}Nb_{0.5}O_3$ and the absence of impurity phases.

Dimensions of the crystallites were estimated using the Debye-Scherrer formula:

$$d = \frac{0.9\lambda}{B\cos\Theta}, \qquad (1)$$

where $\lambda = 0.1542$ nm — the wavelength of X-ray radiation, B — the half-width of the diffraction peak in radians, Θ — the angle that corresponds to the position of the diffraction line on XRD pattern. The calculations showed that an average crystallite size equals 80 nm.

Measurements of Raman spectra were performed on a Raman spectrometer Jobin-Yvon/Horiba, equipped with a confocal mi-

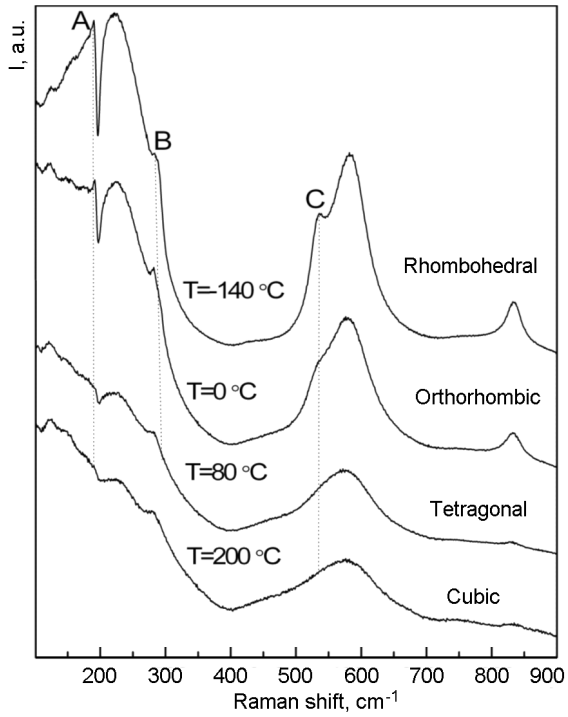

Fig. 1. Temperature dependences of Raman scattering spectra for $KTa_{0.5}Nb_{0.5}O_3$ nanopowder.

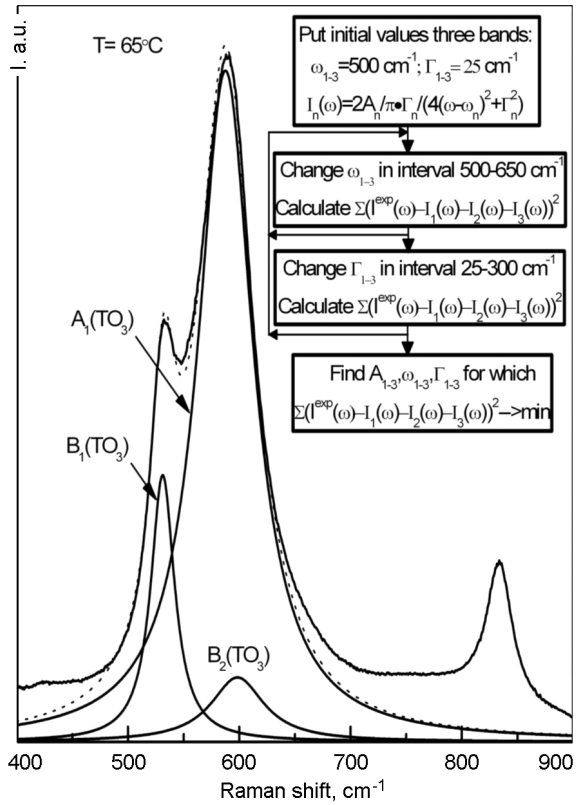

Fig. 2. Decomposition of the experimental wide band in the region 450–750 cm^{-1} into three single Lorentzians.

croscope (lens focal length × 50, NA = 0.60) and CCD detector. An excitation of Raman spectra was performed using Ar^+/Kr^+ laser with a wavelength of 514.5 nm. Input power was no more than 3 mW. The temperature dependence of the spectra within the range from −190°C to 600°C was obtained with the help of a thermoelectric cell Linkam TMS 94. The temperature varied with an interval of 5°C, a rate of 10°C/min and an accuracy of 0.1°C.

3. Results and discussion

Fig. 1 shows the spectra characteristic for the different structural states of $KTa_{0.5}Nb_{0.5}O_3$ powder. In the low-temperature rhombohedral phase, we see the lines of the transverse and longitudinal phonon modes of $B_1(TO_2)$, $A_1(TO_1)$, $B_1(TO_3)$, $A_1(LO_3)$, $A_1(TO_3)$ and $B_2(TO_3)$. Similar phonon modes were observed in the crystals of the solid solutions of KTN in [18]. For further investigation, three transverse optical phonon modes of $B_1(TO_2)$, $A_1(TO_1)$ and $B_1(TO_3)$ were chosen; designated by letters A, B and C, respectively (see Fig. 1).

It is known that during structural phase transitions the phonon modes participating in these transitions condense. At that, during the para- to ferroelectric phase transition, the "condensation of the soft mode" normally means the condensation of the lowest transverse optical mode of the phonon spectrum [19]. In our experiment, we track a mode of $B_1(TO_2)$ (labeled mode A) for a ferroelectric phase transition. Two structural transitions are defined, as will be shown below, by the condensation of modes of $A_1(TO_1)$ and $B_1(TO_3)$, designated by letters B and C, respectively. As visible in Fig. 1, the lines of these modes are narrow at low temperatures, and broaden with the frequency shift as the temperature increases. Unlike lines A and B, changes in line C are difficult to see due to overlap C with lines of $A_1(TO_3)$ and $B_2(TO_3)$ modes. Therefore, before analyzing the spectrum temperature dependence we decompose this part of the spectrum into three single Lorentzians, corresponding to modes of $B_1(TO_3)$, $A_1(TO_3)$ and $B_2(TO_3)$ (Fig. 2).

The algorithm for decomposition of the compound experimental contour is shown on the inset in Fig. 2. At the primary stage, we set the intervals for expected widths (Γ_n) and frequencies (ω_n) of the phonon modes. Then, by tabulating Γ_n and ω_n inside the chosen intervals, we calculate the standard

deviation of the values of the contour sums from the experimental values. At the final stage of the algorithm, we find, among the tabulated values of Γ_n and ω_n, the decomposition of the compound contour for which the standard deviation is minimal. So it is smaller the standard deviation, as it is the more precise and unambiguous the resulting decomposition. The described procedure was done for every experimental temperature. Such way we determined the temperature dependencies of the intensity, width and frequency of each single Lorentzian, corresponding to $B_1(TO_3)$, $A_1(TO_3)$ and $B_2(TO_3)$ modes.

Because no significant anomalies were observed above 150°C, the dependences in Fig. 3 are presented between −200 and 150°C. Now let us analyze these dependences. First, note that the condensation of $B_1(TO_3)$ mode (line C in Fig. 1) leads to its complete disappearance (its integral intensity becomes zero) at a temperature near 30°C. Above this temperature, the given mode becomes unobservable. The width of the line remains practically unchanged at low temperatures, but at 0°C it begins to increase quickly and continues to do so until the line disappears at 30°C. The frequency remains practically unchanged in the interval between −200°C and −50°C, then begins to decrease, from 531 to 528.6 cm^{-1}, and at 0°C begins to increase, reaching 534 cm^{-1} at 30°C. The mode $A_1(TO_3)$ is observed in the entire interval from −200°C to 600°C, but there are significant changes in the slope of the graph in three different regions. The centers of these regions are at −50°C, 30°C, and 86°C. The width of this line doesn't change much between −200°C and 20°C, but if the temperature is further increased, the width increases, with two significant slope changes around 30°C and 86°C. The frequency of the line decreases monotonically between −200°C and −110°C, then has a small jump (from 577 cm^{-1} to 588 cm^{-1}) at −100°C. Above −50°C we once again observe a gradual decrease in frequency, i.e. the condensation of the given mode. The line $B_2(TO_3)$ is similarly observed in the entire investigated temperature range, but its integral intensity does not change, with the exception of a slope change around −100°C. The width and frequency of the given mode also experience a slope change near there. It is likely that the given mode is not nearly sensitive to the three known structural transformations in the material, however it is sensitive

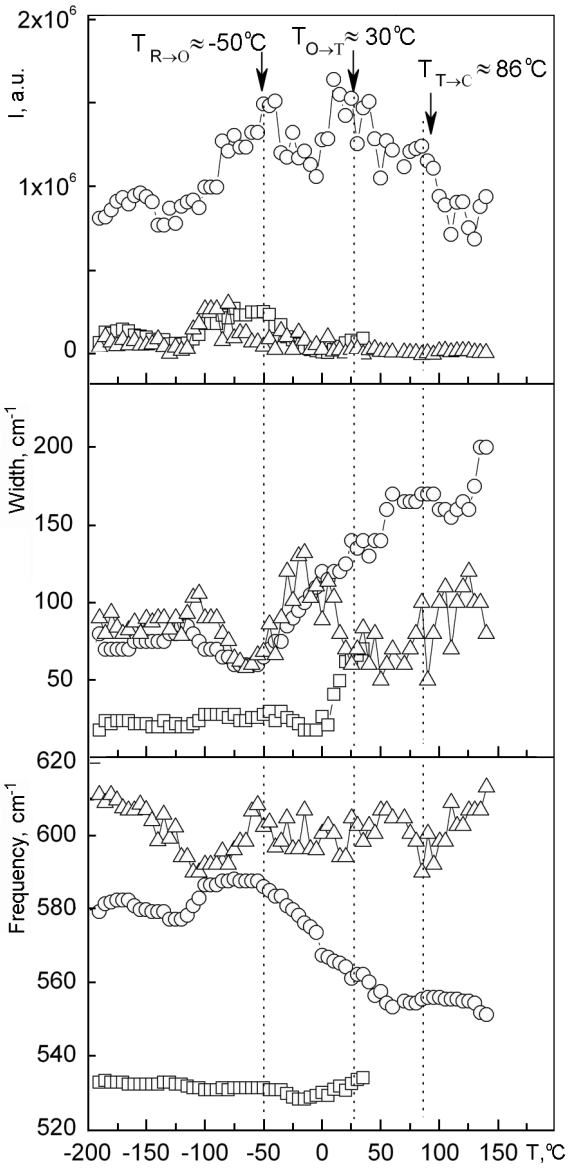

Fig. 3. Temperature dependences of the integrated intensity, width, and frequency of the transverse optical modes $B_1(TO_3)$ (squares), $A_1(TO_3)$ (circles) and $B_2(TO_3)$ (triangles).

to whatever structure change occurs near −100°C. This interesting experimental result requires further investigation. We can speculate that at −100°C there is one additional structural transition, for example, from a rhombohedral to a monoclinic phase. For a more accurate explanation of this phenomenon, an X-ray or neutron-diffraction study is required.

Now let's consider the temperature behavior of the mode $B_1(TO_2)$, i.e. line A in Fig. 1. Dependence of the integrated intensity of this line on temperature is shown in Fig. 4. At low temperatures, there is almost

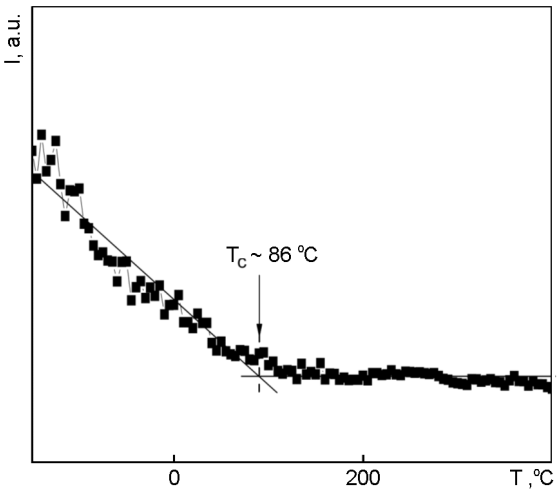

Fig. 4. Temperature dependence of the integrated intensity of $B_1(TO_2)$ mode.

a monotonic decrease of intensity. Starting from about 60°C, the rate of the intensity decreasing slows down and becomes almost zero above 120°C. This interval corresponds to the ferroelectric phase transition. We can definitely say that the range of the phase transition is quite broad; covering more than 60 degrees. We believe that such a wide phase transition interval indicates a large spread of nanopowder particles sizes. Or, in other words, the interval reflects the effect of particle size on the Curie temperature value, so we have a whole set of Curie temperatures, each of which refers to particles of a certain size. The average Curie temperature related to the average size of the particles can be defined as $T_c = 86$°C. Considering that the average particle size, according to the established XRD data, was 80 nm, it can be assumed that T_c refers to particles of this size. The effect of blurring phase transitions because of the spread of particle sizes was earlier observed in work [20] during investigations of the micron-sized $KNbO_3$ powders. The authors attribute this to the fact that different mono-domains near the surface change their orientation at different temperatures. The theoretical calculations of the effect of particle size on T_c also confirm this result. In the temperature dependence of $B_1(TO_2)$ mode frequency the monotonous decrease is noted. At temperatures above 100°C tracking the changes in frequency is almost impossible due to the overlap of the line with the other lines of the spectrum.

Finally, look at the behavior of $A_1(TO_1)$ mode, denoted as line B in Fig. 1. The integrated intesity of this line decreases quickly at higher temperatures and at −50°C it almost reaches zero. Obviously, this branch of the spectrum reflects the dynamics of the structural elements of the lattice, which are involved in the low-temperature phase transitions.

4. Conclusions

The analysis of the temperature dependence of transverse optical modes of the phonon spectrum of $KTa_{0.5}Nb_{0.5}O_3$ nanopowders allows us to make the following conclusion. Characteristic inflections in the temperature dependences of spectroscopic parameters indicate three structural changes in the investigated powders. These rearrangements include a broad temperature range, reflecting the large spread of the powder particles by size. The centers of the intervals correspond to the temperatures — 50°C, 30°C and 86°C. The temperatures of the relevant structural transitions in $KTa_{0.5}Nb_{0.5}O_3$ macrocrystals are −80°C, 20°C and 105°C. Consequently, an average temperature of the area of each of the phase transitions is shifted in different way, in particular: a low-temperature transition 30 degrees higher, a middle transition 10 degrees higher, and the ferroelectric phase transition occurs at 20 degrees lower than the temperature of the corresponding transition in single-crystal $KTa_{0.5}Nb_{0.5}O_3$. In addition, this study reported the sign of a new structural transformation around −100°C. However, its identification requires a further investigation.

References

1. M.G.Cohen, E.I.Gordon, *Appl. Phys. Lett.*, **5**, 181 (1964).
2. F.S.Chen, J.E.Geusic, S.K.Kurtz et al., *J. Appl. Phys.*, **37**, 388 (1966).
3. John A. van Raalte, *J. Opt. Soc. Am.*, **57**, 671 (1967).
4. A.Rousseau, M.Guilloux-Viry, E.Dogheche et al., *J. Appl. Phys.*, **102**, 093106 (2007).
5. X.P.Wang, J.Y.Wang, H.J.Zhang et al., *J. Appl. Phys.*, **103**, 033513 (2008).
6. A.Bartasyte, J.Kreisel, W.Peng, M.Guilloux-Viry, *Appl. Phys. Lett.*, **96**, 262903 (2010).
7. H.-M.Christen, E.D.Specht, D.P.Norton et al., *Appl. Phys. Lett.*, **72**, 2535 (1998).
8. E.D.Specht, H.-M.Christen, D.P.Norton, L.A.Boatner, *Phys. Rev. Lett.*, **80**, 4317 (1998).
9. H.-M.Christen, K.S.Harshavardhan, M.F.Chisholm et al., *J. Electroceram.*, **4**, 279 (2000).
10. S.Triebwasser, *Phys. Rev.*, **114**, 63 (1959).
11. D.A.Tenne, A.Soukiassian, M.H.Zhu et al., *Phys. Rev. B*, **67**, 012302 (2003).

12. K.Y.Zheng, N.Wei, F.X.Yang et al., *Front. Phys. China*, **2**, 436 (2007).
13. Y.M.Hu, H.S.Gu, Z.Hu et al., *Cryst. Grow. Design*, **8**, 832 (2008).
14. Yong-Ming Hu, Hao-Shuang Gu, Di Zhou et al., *J. Am. Ceram. Soc.*, **93**, 609 (2010).
15. O.O.Andriiko, I.V.Kovalenko, L.V.Chernenko et al., *Naukovi Visti NTTU KPI*, No.1, 117 (2008).
16. I.S.Golovina, S. P.Kolesnik, I. N.Geifman, A.A.Andriiko, *Ferroelectrics*, **416**, 133 (2011).
17. I.S.Golovina, S.P.Kolesnik, V.Bryksa et al., *Physica B: Condens. Matter.*, **407**, 614 (2012).
18. G.E.Kugel, H.Mesli, M.D.Fontana, D.Rytz, *Phys. Rev. B*, **37**, 5619 (1988).
19. M.E.Lines, A.M.Glass, Principles and Application of Ferroelectrics and Related Materials, Clarendon Press, Oxford (1977).
20. A.Baier-Saip, E.Ramos-Moor, A.L.Cabrera, *Solid State Communications*, **135**, 367 (2005).

Дослідження фазових переходів у нанопорошку $KTa_{0.5}Nb_{0.5}O_3$ методом Романівської спектроскопії

І.С.Головіна, В.П.Брикса, В.В.Стрельчук, І.Н.Гейфман

Вперше отримано і досліджено Раманівські спектри нанопорошків твердого розчину $KTa_{0.5}Nb_{0.5}O_3$ у діапазоні температур $-190°C<T<600°C$. Матеріал синтезировано за новою технологією. Температурні залежності інтенсивності, ширини і частоти мод $B_1(TO_2)$, $A_1(TO_1)$, $B_1(TO_3)$, $A_1(TO_3)$ і $B_2(TO_3)$ ретельно проаналізованіо. Зареєстровано суттєве розмиття областей усіх фазових переходів, пов'язане із розкидом часток за розмірами. Встановлено, що середні температури областей кожного з фазових переходів зсуваються по різному, а саме: низькотемпературний перехід реалізується на 30 градусів вище, середній — на 10 градусів вище, а сегнетоелектричний перехід відбувається на 20 градусів нижче температур відповідних переходів у монокристалах $KTa_{0.5}Nb_{0.5}O_3$.